Highly efficient and selective removal of tetracycline from aqueous solutions via adsorption onto Cu(II)-modified hierarchical ZSM-5

Subing Fan, Junmin Lv, Yulong Ma and Yaoyao Chen

ABSTRACT

Herein, we prepared Cu(II)-modified hierarchical ZSM-5 containing both micro- and mesopores by alkali treatment followed by ion exchange as an adsorbent, using it for tetracycline (TC) removal from aqueous solutions. The crystal structure, morphology, texture, and Si:Al ratio of this adsorbent by a range of instrumental techniques were investigated. Moreover, we studied the effect of pH and Cu(II) loading on adsorption performance and probed adsorption kinetics, thermodynamics and regeneration performance, revealing that modification of hierarchical ZSM-5 with Cu(II) not only significantly increased its TC removal efficiency but also allowed for good regenerability and suggested that the highly efficient and selective removal of TC from aqueous solutions could be ascribed to not only the strong interactions between Cu(II) and TC molecular but also the larger mesoporosity.

Key words | adsorption, mesopore, molecular sieve, regeneration, tetracycline

Subing Fan
Junmin Lv
Yulong Ma (corresponding author)
Yaoyao Chen
State Key Laboratory of High-efficiency Utilization of Coal and Green Chemical Engineering, College of Chemistry and Chemical Engineering,
Ningxia University,
Yinchuan, 750021,
China
E-mail: *yulongma796@sohu.com*

INTRODUCTION

Pharmaceutical antibiotics are broadly used worldwide for agricultural purposes as well as for controlling bacterial infections in humans and animals (Le-Minh *et al.* 2010; Li *et al.* 2014). Most antibiotics, including tetracycline (TC), cannot be metabolized or absorbed *in vivo* and are generally excreted into the environment through urine or feces as maternal forms (Gao *et al.* 2012). In the case of TC, excreted residues subsequently enter soil and groundwater, and can even find their way into drinking water. Therefore, the discharge of TC-containing wastewater by pharmaceutical industry poses a potential threat to the ecosystem and human health in view of the acute or chronic toxicity of TC and the possible evolution of TC-resistant microorganisms (Brigante & Schulz 2011). The stable structure and hydrophilic character of TC (Daghrir & Drogui 2013) hinder its removal from the environment via natural degradation (Becker *et al.* 2016); moreover, oxidative degradation is poorly suited for the complete removal of TC from aqueous solutions and can generate metabolites or degradation products with an even more serious environmental impact (Martínez-Huitle & Ferro 2006; Homem & Santos 2011). In addition, the applicability of oxidative degradation is limited by the small flow rate and the high operating cost of corresponding reactors (Homem & Santos 2011), while the ease of membrane blockage and high energy consumption hinder the large-scale application of membrane separation, photocatalytic, and electrochemical processes (Homem & Santos 2011; Pulido 2016). Finally, antibiotics cannot be effectively biodegraded or can be biodegraded only in very low concentrations because of their toxicity to microorganisms and unfriendly environment (Zhang *et al.* 2018).

Fortunately, adsorption-based removal techniques using suitable adsorbent generally do not cause secondary pollution and allow for adsorbent re-use, which results in decreased costs and lower energy consumption (Yu *et al.* 2016). Adsorbent is the key of the adsorption method. Although the adsorption technique developed well in recent years, for conventional adsorbent including active carbon, silica gel, biomass, solid waste and so on, there still exist many problems that need to be researched and resolved, especially for biosorbents, such as non-selective adsorption, mass loss of pretreatment, biodegradable or decomposable in adsorption processes, low thermal stability, difficult regeneration and disposing, and unassured supply of biomass (Park *et al.* 2010; El-sayed & El-sayed 2014). However, adsorbent of molecular sieve is far away from almost all of these troubles.

doi: 10.2166/wst.2019.099

Molecular sieves with an ordered pore structure and large specific surface area commonly exhibit excellent catalytic and adsorption performances and are widely applied in many fields such as agriculture and industry (Groen *et al.* 2007; Choi *et al.* 2013). Among the numerous parameters of adsorbents, cation exchange capacity is particularly important, since the increase of this capacity allows the introduction of a greater number of selective adsorption sites for enhanced adsorption performance (Parolo *et al.* 2008). Moreover, because of their excellent (hydro)thermal stability, most molecular sieves exhibit regenerabilities superior to those of other materials and are therefore well suited for pollutant removal via adsorption. Depending on solution pH, TC can exist in cationic, zwitterionic, or anionic forms (Brigante & Schulz 2011), and the corresponding electron-donating residue can easily coordinate divalent metal ions (MacKay & Canterbury 2005; Jin *et al.* 2007), with one of the highest binding energies observed for Cu(II) (Figueroa *et al.* 2004; Pils & Laird 2007; Wang *et al.* 2008). Wang *et al.* studied the effect of Cu(II) ions on the adsorption of TC from aqueous solution onto montmorillonite, revealing that the efficiency of the above adsorption increased in the presence of Cu(II) in a certain pH range (Wang *et al.* 2008), which confirmed that TC and Cu(II) ions engage in strong interactions.

The above results seem to suggest that the TC adsorption efficiency of a given adsorbent should increase upon its modification with Cu(II). However, although microporous molecular sieves feature high ion exchange capacities (and hence, abundant potential adsorption sites), their small pore size severely limits TC adsorption performance, and most TC molecules are adsorbed on the smaller external surface (Groen *et al.* 2007; Abelló *et al.* 2009). On the other hand, most mesoporous molecular sieves, which have a larger pore size, are purely siliceous and feature fewer adsorption sites, which restricts selective adsorption (Shah *et al.* 2015).

To address this issue, we herein modified a hierarchical ZSM-5 molecular sieve, which features both abundant active adsorption sites and large mesopore volume, with Cu(II) ions and studied the fundamental TC adsorption behavior, adsorption kinetics, and regenerability of this modified adsorbent.

MATERIALS AND METHODS

Materials

Tetracycline hydrochloride (AR) was purchased from J&K Scientific Ltd and stored in the dark at 4 °C. Commercial NaOH (AR) and $Cu(NO_3)_2{\cdot}3H_2O$ (AR) were purchased from Sinopharm Chemical Reagent Co., Ltd (China) and used as received. Microporous molecular sieves (ZSM-5) were purchased from Nanjing Huangma Chemical Co., Ltd (China).

Preparation procedures

Preparation of hierarchical ZSM-5

Based on the desilication principle, ZSM-5 with SiO_2/Al_2O_3 (mol/mol) = 30 was selected. Aqueous NaOH (0.1, 0.5, and 1.0 M) was used as a reagent for alkali treatment. The solid–liquid ratio was set to 1 g: 20 mL, and the alkali treatment temperature was set to 90 °C. Dried ZSM-5 (3 g) was exposed to aqueous NaOH for 1 h, filtered off, thoroughly washed with water until the filtrate pH reached 8.0, and dried to afford hierarchical ZSM-5(A,*x*), where A represents alkali treatment and *x* represents the concentration of NaOH (Shen *et al.* 2012; Kustov *et al.* 2018).

Modification of ZSM-5(A) with Cu(II) via ion exchange

ZSM-5(A) was added to $Cu(NO_3)_2$ solutions (100 mL) of different concentrations to achieve $Cu(NO_3)_2$:ZSM-5(A) mass ratios of 0, 0.1, 0.5, 1.0, 1.5, or 2.0 $g\,g^{-1}$, and the obtained suspensions were refluxed for 3 h at 80 °C upon stirring and filtered. The solid was washed with hot demineralized water until no Cu(II) was detected in the filtrate. The ion exchange process was repeated three times, and the resulting samples were oven-dried at 80 °C overnight (Salama & Ahmed 2006; Fathima *et al.* 2008) and denoted as Cu(*y*)-ZSM-5(A,*x*), where *y* represents the $Cu(NO_3)_2$: ZSM-5(A) mass ratio ($g_{Cu(NO3)2}\ g^{-1}_{ZSM\text{-}5(A)}$).

Characterization and analysis

X-ray diffraction (XRD; Rigaku D/Max 2200) patterns of ZSM-5, ZSM-5(A), and Cu-ZSM-5(A) samples were recorded using Ni-filtered Cu K_α radiation at 30 kV and 20 mA, and scanning was performed from 3 to 60° at 8° min^{-1} in steps of 0.02°. ZSM-5(A) was additionally characterized by transmission electron microscopy (TEM; JEM-2100F), and the content of Cu(II) was analyzed by energy-dispersive X-ray fluorescence (XRF; S2 RANGER). The surface area, pore volume, and pore size distribution of synthesized samples were analyzed by N_2 adsorption–desorption measurements (JW-BK132F).

Adsorption experiments

Typically, a flask was charged with a TC solution of the desired concentration (100 mL), and pH was adjusted using NaOH (0.10 M for TC concentrations of 50–200 mg L^{-1} and 1.0 M for a TC concentration of 400 mg L^{-1}) at 308 K. Next, the above solution was treated with 0.040 g of ZSM-5, ZSM-5(A), or Cu-ZSM-5(A) with different Cu(II) loadings. The flask was sealed with Al foil, put into a thermostatic oscillator, and the above suspension was continuously stirred in the dark at 120 rpm. Approximately 0.1-mL filtrate samples were extracted from the flask at regular intervals using a 0.22-μm membrane until adsorption equilibrium was reached, and the TC removal performance was analyzed by HPLC. The equilibrium TC adsorption capacity was calculated using Equation (1) (Choi *et al.* 2008):

$$q_e = (C_0 - C_e)V/M \quad (1)$$

where q_e (mg g^{-1}) is the equilibrium TC adsorption capacity of ZSM-5, C_0 and C_e (mg L^{-1}) are the initial and equilibrium concentrations of TC, respectively; V (L) is the volume of the aqueous solution, and W (g) is the adsorbent mass.

Adsorption kinetics

To probe TC adsorption kinetics, experiments were conducted at initial TC concentrations of 50, 100, 200, and 400 mg L^{-1}, a Cu(1.0)-ZSM-5(A,0.5) dosage of 0.04 g, a temperature of 35 °C, and an initial pH of 7.0. A blank experiment was carried out using non-modified ZSM-5.

Three kinetic models (pseudo-first-order, pseudo-second-order, and intra-particle diffusion models) were used to fit experimental data (Ho 1995; Ho & McKay 1999):

$$\text{Pseudo-first-order model: } \ln(q_e - q_t) = \ln q_e - k_1 t \quad (2)$$

$$\text{Pseudo-second-order model: } t/q_t = 1/(k_2 q_e^2) + t/q_e \quad (3)$$

$$\text{Intra-particle diffusion model: } q_t = k_3 t^{0.5} + C \quad (4)$$

where k_1 (min^{-1}) is the first-order rate constant, k_2 (mg g^{-1} min^{-1}) is the second-order rate constant, k_3 (mg g^{-1} $min^{-0.5}$) is the intra-particle diffusion rate constant, C (mg g^{-1}) is a constant reflecting boundary layer thickness, and q_e and q_t (mg g^{-1}) are TC adsorption capacities at equilibrium and at time t (min), respectively.

Adsorption thermodynamics

Thermodynamic equilibrium constant K was calculated using the method of Khan and Raji (Khan & Singh 1987; Raji & Anirudhan 1998) based on a series of experimental results with different concentrations of TC and different adsorption temperatures. The standard free energy change ΔG_0, the enthalpy change ΔH and entropy change ΔS follow the equations:

$$\Delta G_0 = -\mathrm{RT}\ln K \quad (5)$$

$$\ln K = -\Delta H/(RT) + \Delta S/R \quad (6)$$

Regeneration experiments

Cu(1.0)-ZSM-5(A,0.5) (0.5 g) and TC solution (500 mL, 1,000 mg L^{-1}) reacted as described above. When a close-to-saturation state was reached (removal efficiency >95%), the adsorbent was carefully filtered off, heated for 2 h at 300 °C in air to remove adsorbed TC, and used in subsequent experiments. This regeneration–adsorption process was repeated four times.

RESULTS AND DISCUSSION

Characterization of ZSM-5(A)

Morphology

Figure 1 shows the morphology of alkali-treated ZSM-5(A,0.5), demonstrating that, in contrast to ZSM-5 crystals with a smooth surface, ZSM-5(A,0.5) featured numerous mesopores (intra-mesopores) with non-uniform size. Thus, alkali treatment of ZSM-5 resulted in efficient mesopore formation and was therefore expected to benefit TC removal performance.

Texture

Figure 2(a) shows the adsorption–desorption isotherms and Figure 2(b) shows mesopore distribution of ZSM-5(A,0.5). An obvious hysteresis loop was observed at $P/P_0 = 0.25$–0.95, which indicated the formation of mesopores. Based on the obtained results in Figure 2(b), the most probable pore diameters were determined to be 2.3 and 3.9 nm.

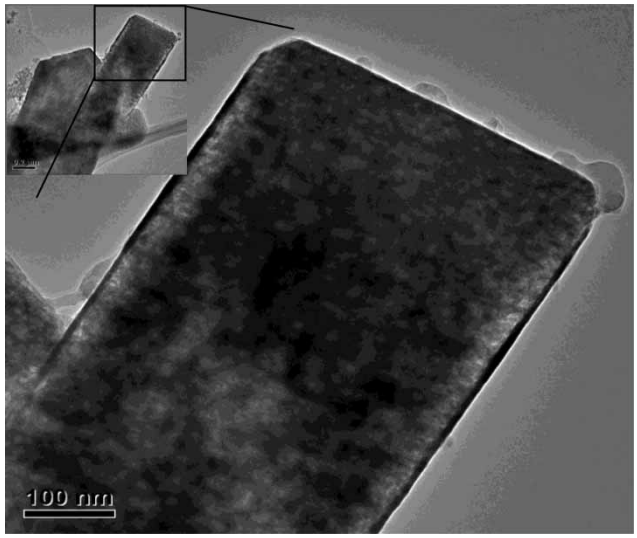

Figure 1 | The TEM image of ZSM-5(A,0.5).

Table 1 lists the textural properties of ZSM-5 and ZSM-5(A), showing that alkali treatment of the former resulted in a marked property change, e.g. in the formation of mesopores in the originally microporous ZSM-5. With increasing NaOH concentration, the internal specific surface area slightly decreased, while the external specific surface area sharply increased, except for in the case of 1.0 M NaOH. Likewise, micropore volume remained almost unchanged after alkali treatment, while the mesopore volume increased (except for the abovementioned case), and the average mesopore size after alkali treatment reached 3.9 nm. Thus, at moderate NaOH concentration, the microporosity of all samples remained almost unaffected, and sample mesopore volume and external specific surface area could be adjusted by variation of treatment conditions, which suggested that controlled formation of intramesopores could be achieved to further improve the affinity of the adsorbent to large molecules such as TC. At an NaOH concentration of 1 M, both the internal specific surface area and micropore volume sharply declined, which indicated that the micropore texture of ZSM-5 was destroyed at an overly high alkali concentration. In contrast, after treatment with 0.5 M NaOH, the mesopore volume of ZSM-5 increased from 0.095 to 0.294 $cm^3 g^{-1}$, and the external specific surface area increased from 44 to 110 $m^2 g^{-1}$.

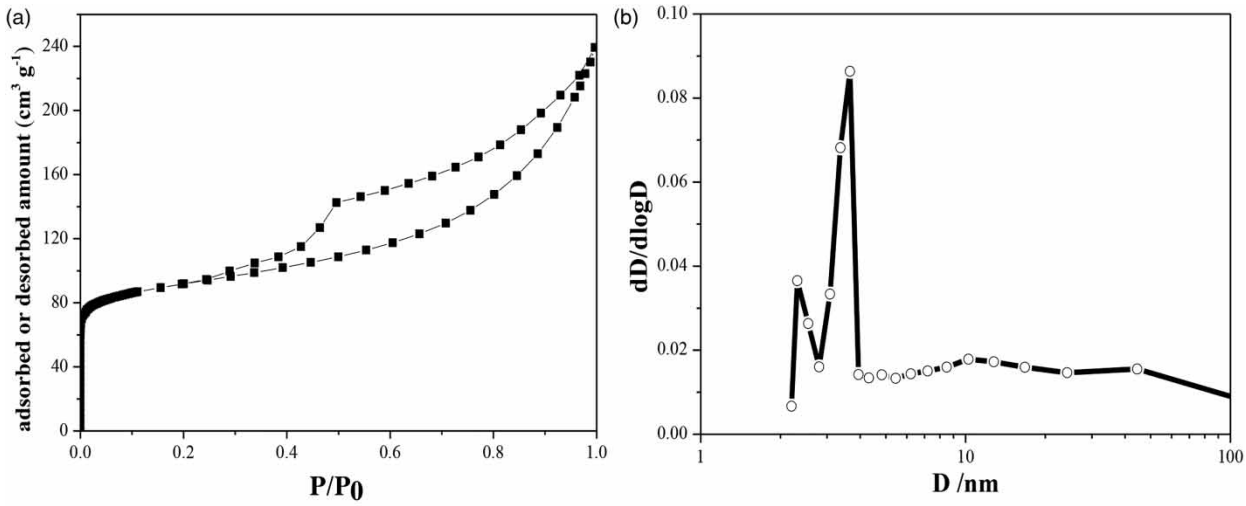

Figure 2 | (a) The adsorption–desorption isotherms and (b) mesopore distribution of ZSM-5(A,0.5).

Table 1 | The textural properties of ZSM-5 and ZSM-5(A)[a]

	S_{int}($m^2 g^{-1}$)	S_{ext} ($m^2 g^{-1}$)	S_{total} ($m^2 g^{-1}$)	V_{meso} ($cm^3 g^{-1}$)	V_{micro} ($cm^3 g^{-1}$)	D_{meso} (nm)
ZSM-5	310.8	44.1	354.9	0.095	0.11	2.3
ZSM-5(A,0.1)	286.5	64.8	351.3	0.110	0.11	3.8
ZSM-5(A,0.5)	248.4	110.0	358.4	0.294	0.13	3.9
ZSM-5(A,1.0)	37.0	77.1	114.1	0.262	0.04	3.9

[a]S_{int}: internal specific surface area; S_{ext}: external specific surface area; S_{total}: total specific surface area; V_{micro}: micropore volume; V_{meso}: mosopore volume; D_{meso}: average mesopore size.

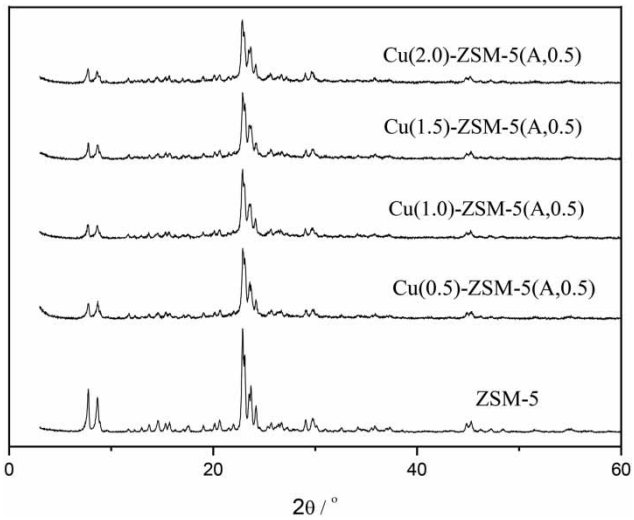

Figure 3 | XRD patterns of ZSM-5 and Cu-ZSM-5(A,0.5) with different Cu(II) loading.

Characterization of Cu(II)-modified ZSM-5(A,0.5)

Cu(II) loading

To investigate the influence of Cu(II) loading on the crystal structure of ZSM-5(A,0.5), samples obtained at $Cu(NO_3)_2$: ZSM-5(A,0.5) mass ratios of 0, 0.1, 0.5, 1.0, 1.5, and 2.0 g g^{-1} were characterized by XRD (Figure 3). Notably, the intensity of characteristic Cu-ZSM-5(A,0.5) peaks decreased with increasing Cu(II) loading, but the skeleton structure of ZSM-5 was well maintained after desilication and Cu(II) introduction.

Si:Al ratios (SARs)

Table 2 lists the SARs of ZSM-5, ZSM-5(A,0.5), and Cu-ZSM-5(A,0.5), determined by XRF, demonstrating that alkali treatment reduced the SAR of ZSM-5 from 34.7 to 15.3, which was ascribed to desilication and partial destruction, in accordance with the abovementioned changes in morphology, specific surface area, and characteristic peak intensity. This finding simultaneously indicated that the ion exchange capacity of ZSM-5 increased after alkali treatment, which allowed more Cu(II) ions to be incorporated into ZSM-5(A) to increase the TC removal efficiency. However, the SAR was almost independent of Cu(II) loading, and ion exchange was therefore concluded to only weakly influence the above ratio.

Table 2 | The SARs of ZSM-5, ZSM-5(A,0.5), and Cu-ZSM-5(A,0.5)

	ZSM-5	ZSM-5(A,0.5)	Cu-ZSM-5-(A,0.5)				
Cupric nitrate/g g_{ZSM-5}^{-1}	0	0	0.1	0.5	1.0	1.5	2.0
SAR	34.7	15.3	15.8	17.4	14.4	17.6	13.6

Adsorption performance

Effect of pH

Figure 4 shows the effect of pH on the efficiency of TC (50 mg L^{-1}) removal by Cu(1.0)-ZSM-5(A,0.5), demonstrating that adsorption was more efficient under neutral and weakly alkaline conditions than under strongly acidic or alkaline ones. In particular, the highest removal efficiency of 98.8% was observed at pH 7.0.

The above behavior was explained by the influence of pH on the ionization state of TC and on the stability of ZSM-5(A,0.5). Specifically, pH-dependent protonation–deprotonation transitions of TC functional groups resulted in the transformation of neutral TC molecules into zwitterionic species. Moreover, Cu(II) ions loaded onto the surface of ZSM-5 could be back-exchanged for H^+ ions at pH <7.0, which resulted in the loss of active adsorption sites on the surface of ZSM-5(A,0.5) and promoted the formation of soluble TC-Cu(II) complexes. Additionally, adsorbent dealuminization was highly likely to occur at overly low pH, while desilication of the Cu-ZSM-5(A,0.5) framework was likely under strongly alkaline conditions. In both of these extreme scenarios, Cu(II) ions were leached into the solution, which greatly decreased the TC adsorption

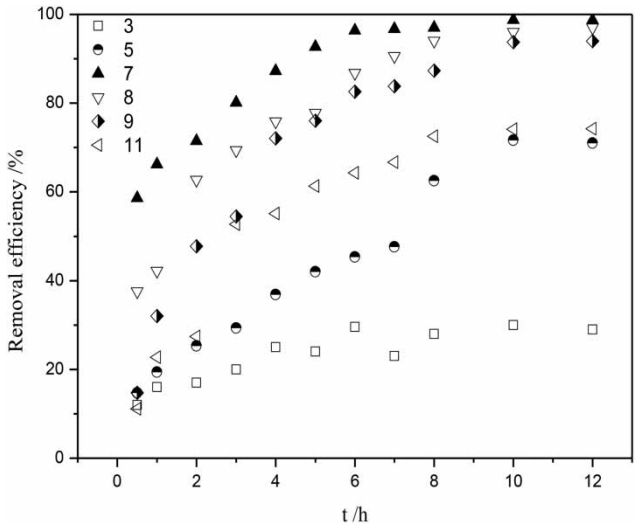

Figure 4 | Effect of solution pH on removal efficiency of Cu(1.0)-ZSM-5(A,0.5).

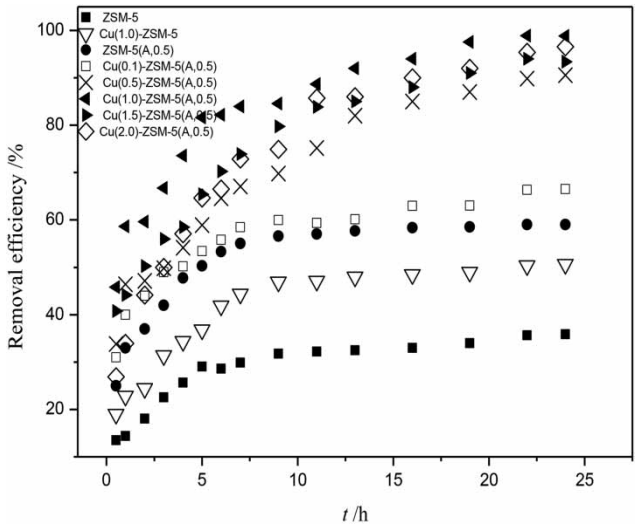

Figure 5 | The removal efficiency of Cu-ZSM-5(A,0.5) with different Cu(II) loading.

capacity of Cu-ZSM-5(A,0.5). Therefore, solution pH was considered to be a crucial parameter determining the stability of molecular sieve-type adsorbents.

Effect of Cu(II) loading

Cu-ZSM-5(A,0.5) (0.04 g) was added to a solution of TC (100 mL, 100 mg L^{-1}), and solution pH was adjusted to 7.0 with 0.1 M NaOH. Figure 5 shows the resulting time profile of TC removal efficiency, while Table 3 shows both the Cu(II) content and corresponding equilibrium removal efficiency. The removal efficiency rapidly increased in the beginning, subsequently slowing down and finally reaching equilibrium. Notably, the TC removal efficiencies of only Cu(II)-exchanged and only alkali-treated ZSM-5 (51% and 59%, respectively) exceeded that of pristine ZSM-5 (36%), which suggested that for only-micropore-containing ZSM-5, TC removal efficiency could be increased by the formation of active adsorption sites or mesopores. Notably, the removal efficiency increased even further when ZSM-5 was subjected to both alkali treatment and Cu(II) ion exchange, reaching a maximal value of 98.8% at a Cu(II) loading of 1.0 g $g^{-1}_{ZSM\text{-}5(A)}$. Thus, the latter parameter was an important factor affecting TC adsorption efficiency, and Cu(II) ions were present at active adsorption sites. When the Cu(II) loading increased further, the amount of ion-exchanged sites on ZSM-5(A) remained almost constant, which suggested that the excellent adsorption performance originated from the cooperative effect of Cu(II) and mesopores. At this point, it is worth noting that at Cu(II) loadings exceeding 0.5 g $g^{-1}_{ZSM\text{-}5(A)}$, the establishment of adsorption equilibrium took a long time (>25 h), which was attributed to the conflict between (i) the increase of adsorption capacity caused by the increase of the number of active adsorption sites and (ii) the diffusion rate of TC accessing the active adsorption sites inside the pores of Cu-ZSM-5(A,0.5).

Kinetics of TC adsorption on Cu(1.0)-ZSM-5(A,0.5)

Considering crystallinity and removal efficiency, Cu(1.0)-ZSM-5(A,0.5) was selected as an optimal adsorbent for kinetic experiments. Pseudo-first-order and intra-particle diffusion models did not reliably reproduce experimental data, as reflected by small correlation coefficient (R^2) values and large differences between calculated and experimental adsorption capacities. Conversely, the pseudo-second-order model reliably reproduced experimental data obtained at four initial TC concentrations (50, 100, 200, and 400 mg L^{-1}), as shown in Figure 6 and Table 4, achieving R^2 values above 0.99. They thus predicted q_e values were in good agreement with experimental results. Notably, the adsorption mechanism was suggested to resemble that of TC selective adsorption on Cu-13X depending on the strong complexation of Cu(II) with NH_2 radical of amide group in TC (similar dynamic model and similar material) (Lv *et al.* 2015). The adsorption efficiency was concluded to be determined by the interactions between Cu(II) ions in hierarchical ZSM-5 and TC molecules as well as by the presence of large mesopores, which provided the space required for the access of the above molecules.

Table 3 | The Cu(II) content and corresponding equilibrium removal efficiency

	ZSM-5	Cu-ZSM-5	ZSM-5(A,0.5)	Cu-ZSM-5(A,0.5)				
Cupric nitrate/g g^{-1}_{ZSM-5}	0	0	0	0.1	0.5	1	1.5	2
Real Cu(II) content/%	0	0	0	5.43	7.14	8.03	7.78	7.98
Removal efficiency/%	35.8	50.7	59	66.5	90.5	98.8	94	96.6

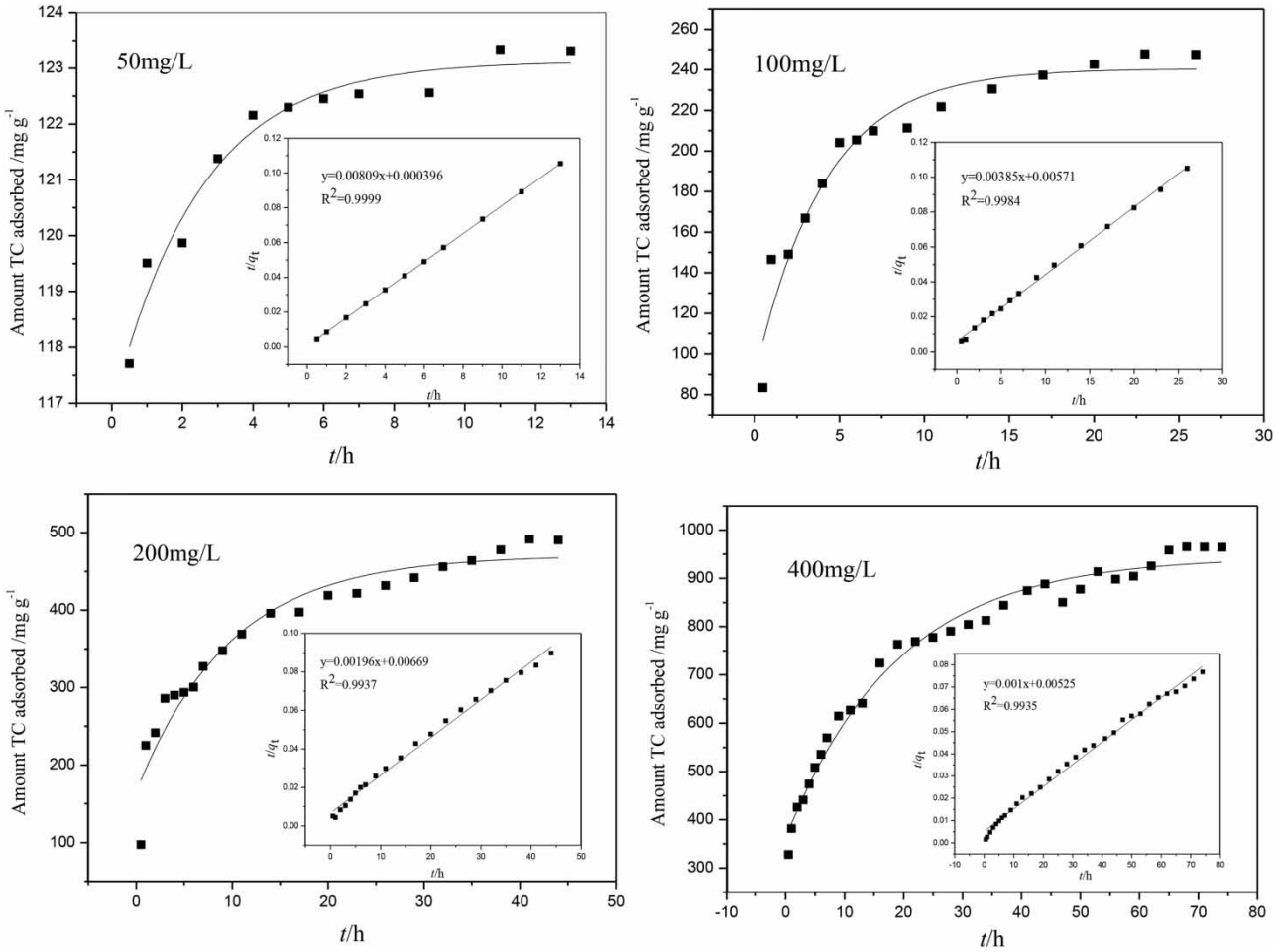

Figure 6 | Kinetics of TC adsorption and linear fitted by pseudo-second-order kinetics model (inset).

Adsorption thermodynamics

The adsorption thermodynamic parameters were calculated according to a series of experimental results and showed in Table 5. The value of equilibrium constant K is small and decreased with the adsorption temperature, suggesting the adsorption rate is slow and the adsorption process was an exothermic process agreeing with the negative value of ΔH (-18.5 kJ mol^{-1}) which indicating the physisorption. The adsorption rate is not only relative to diffusion rate of TC in solution, but also depends on the complexation rate. Although both the concentration of TC in solution and Cu(II) ions on ZSM-5 are relative low, resulting the low diffusion rate or low contact frequency, the rate of complexation between Cu(II) ions and TC molecular is lower. At that moment, the adsorption rate depended on the complexation rate. Following Equation (5), the ΔG is negative and its absolute value (ca. 13 kJ mol^{-1}) is also small, indicating the adsorption process was spontaneous and the initial driving force of adsorption is not very high. The negative value of ΔS revealed the nature of adsorption from disorder to

Table 4 | The fitted parameters of pseudo-second-order kinetic model

C_0/mg L^{-1}	q_e/mg g^{-1}	$K_2 \times 10^{-4}$/g mg^{-1} min^{-1}	R^2
50	123.61	1,652.42	0.9999
100	259.74	25.96	0.9984
200	510.20	5.74	0.9937
400	1,000.00	1.90	0.9935

Table 5 | Calculated thermodynamic parameters

T/K	K	ΔG/kJ mol^{-1}	ΔS/J mol^{-1} K^{-1}	ΔH/kJ mol^{-1}	R^2
298	192	−13.5	− 16.9	− 18.5	0.9990
308	181	−13.3			
318	178	−13.1			

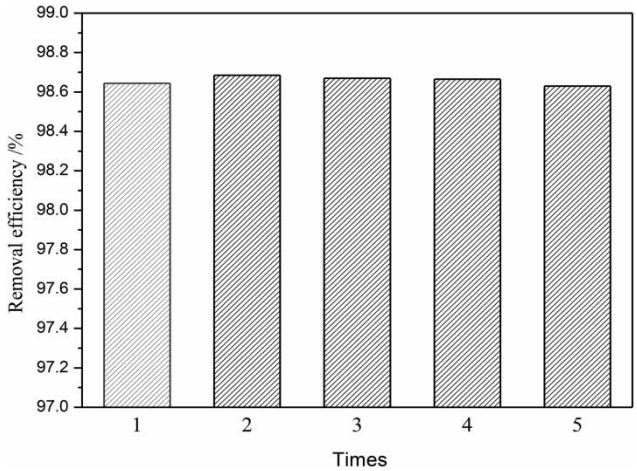

Figure 7 | Regenerability of Cu(1.0)-ZSM-5(A,0.5).

order due to the interaction between TC molecular and adsorbent.

Regeneration of Cu(1.0)-ZSM-5(A,0.5)

Figure 7 summarizes the results of experiments that were carried out to assess the regenerability of Cu(1.0)-ZSM-5(A,0.5). In accordance with our previous studies (Lv *et al.* 2015; Lv *et al.* 2017), which revealed that the maximum adsorption capacity of ZSM-5 may reach ~2,000 mg g^{-1}, the maximum adsorption capacity determined herein reached at least 1,000 mg g^{-1} (Table 4). Therefore, adsorbent regenerability was tested at a 1:1 (w/w) TC:adsorbent ratio. To our delight, the efficiency of TC removal remained as high as 98.6% after four rounds of adsorption–regeneration, which indicated that Cu(1.0)-ZSM-5(A,0.5) exhibited excellent regenerability. ZSM-5 is well known to exhibit high (hydro)thermal stability. For example, many catalytic reactions such as methanol-to-propylene (MTP), methanol-to-aromatics, catalytic cracking, and other transformations are carried out at temperatures above 550 °C because of the high stability of the corresponding molecular sieve catalysts (e.g. the lifetime of an industrial MTP catalyst exceeds two years), which lose Al in preference to undergoing framework degradation. Thus, ZSM-5 was expected to exhibit a very long lifetime and excellent regenerability under the employed adsorption ($T < 40$ °C) and calcination ($T = 300$ °C) conditions.

CONCLUSIONS

Herein, we used alkali treatment followed by ion exchange to prepare hierarchical Cu-ZSM-5 as an adsorbent for highly efficient and selective TC removal. Modification of ZSM-5 to afford ZSM-5(A,0.5) resulted in a total pore volume increase from 0.095 to 0.294 $cm^3\ g^{-1}$ and an external surface area increase from 44.1 to 110 $m^2\ g^{-1}$, while the efficiency of TC removal increased from 35.8 to 98.8% upon going from ZSM-5 to Cu(1.0)-ZSM-5(A,0.5) for a solution with TC of 100 mg L^{-1}(100 mL). Importantly, adsorption performance was largely determined by the co-presence of Cu(II) ions and large mesopores. The adsorption process was well fitted by a pseudo-second-order kinetic model. The equilibrium constant K is low and the adsorption of TC on Cu(II)-modified ZSM-5 was a spontaneous and exothermic process. Moreover, Cu(II)-modified ZSM-5 exhibited good regenerability and potentially good (hydro)thermal stability, i.e. was easy to separate and featured the advantages of high efficiency, reusability, low cost, green nature, and sustainability. As mentioned above, the combined action of Cu(II) ions and mesopores significantly influenced adsorption performance, and the long time required to reach adsorption equilibrium suggested that the presence of large mesopores alone is not sufficient for fast adsorption, demonstrating that adsorbents with more mesopores or larger external surface areas need to be developed.

ACKNOWLEDGEMENT

Financial supports from the National Natural Science Foundation of China (No. 21467023), the Scientific Research Foundation of the Higher Education Institutions of Ningxia (NGY2016005, NGY2017001), and the National First-rate Discipline Construction Project of Ningxia (Chemical Engineering & Technology, NXYLXK2017A04) are greatly acknowledged.

REFERENCES

Abelló, S., Bonilla, A. & Pérez-Ramírez, J. 2009 Mesoporous ZSM-5 zeolite catalysts prepared by desilication with organic hydroxides and comparison with NaOH leaching. *Applied Catalysis A: General* **364**, 191–198.

Becker, D., Giustina, S. V. D., Rodriguez-Mozaz, S., Schoevaart, R., Barceló, D., Cazes, M. D., Belleville, M.-P., Sanchez-Marcano, J., Gunzburg, J. D., Couillerot, O., Völker, J., Oehlmann, J. & Wagner, M. 2016 Removal of antibiotics in wastewater by enzymatic treatment with fungal laccase – degradation of compounds does not always eliminate toxicity. *Bioresource Technology* **219**, 500–509.

Brigante, M. & Schulz, P. C. 2011 Remotion of the antibiotic tetracycline by titania and titania–silica composed materials. *Journal of Hazardous Materials* **192**, 1597–1608.

Choi, K. J., Kim, S. G. & Kim, S. H. 2008 Removal of tetracycline and sulfonamide classes of antibiotic compound by powdered activated carbon. *Environmental Technology* **29**, 333–342.

Choi, K., Na, M. & Ryoo, R. 2013 Recent advances in the synthesis of hierarchically nanoporous zeolites. *Microporous and Mesoporous Materials* **166**, 3–19.

Daghrir, R. & Drogui, P. 2013 Tetracycline antibiotics in the environment: a review. *Environmental Chemistry Letters* **11**, 209–227.

El-Sayed, H. E. M. & El-Sayed, M. M. H. 2014 Assessment of food processing and pharmaceutical industrial wastes as potential biosorbents: a review. *Biomed Research International* **8**, 146769.

Fathima, N. N., Aravindhan, R. & Rao, J. R. 2008 Dye house wastewater treatment through advanced oxidation process using Cu-exchanged Y zeolite: a heterogeneous catalytic approach. *Chemosphere* **70**, 1146–1151.

Figueroa, R. A., Leonard, A. & Mackay, A. A. 2004 Modeling tetracycline antibiotic sorption to clays. *Environmental Science & Technology*. **38**, 476–483.

Gao, Y., Li, Y., Zhang, L., Huang, H., Hua, J. J., Shah, S. M. & Su, X. G. 2012 Adsorption and removal of tetracycline antibiotics from aqueous solution by graphene oxide. *Journal of Colloid and Interface Science* **368**, 540–546.

Groen, J. C., Moulijn, J. A. & Pérez-Ramírez, J. 2007 Alkaline posttreatment of MFI zeolites from accelerated screening to scale-up. *Industrial & Engineering Chemistry Research* **46**, 4193–4201.

Ho, Y. S. 1995 *Adsorption of Heavy Metals From Waste Streams by Peat*. PhD Thesis, The University of Birmingham, Birmingham, UK.

Ho, Y. S. & McKay, G. 1999 Comparative sorption kinetic studies of dye and aromatic compounds onto fly ash. *Journal of Environmental Science and Health* **34**, 1179–1204.

Homem, V. & Santos, L. 2011 Degradation and removal methods of antibiotics from aqueous matrices – a review. *Journal of Environmental Management* **92**, 2304–2347.

Jin, L., Amaya-Mazo, X., Apel, M. E., Sankisa, S. S., Johnson, E., Zbyszynska, M. A. & Han, A. 2007 Ca^{2+} and Mg^{2+} bind tetracycline with distinct stoichiometries and linked deprotonation. *Biophysical Chemistry* **128**, 185–196.

Khan, A. A. & Singh, R. P. 1987 Adsorption thermodynamics of carbofuran on Sn(IV) arsenosilicate in H^+, Na^+ and Ca^{2+} forms. *Colloids and Surfaces* **24**, 33–42.

Kustov, L., Golubeva, V., Korableva, A., Anischenko, O., Yegorushina, N. & Kapustin, G. 2018 Alkaline-modified ZSM-5 zeolite to control hydrocarbon cold-start emission. *Microporous and Mesoporous Materials* **260**, 54–58.

Le-Minh, N., Khan, S. J., Drewes, J. E. & Stuetz, R. M. 2010 Fate of antibiotics during municipal water recycling treatment processes. *Water Research* **44**, 4295–4323.

Li, Y. F., Zhu, G. B., Ng, W. J. & Tan, S. K. 2014 A review on removing pharmaceutical contaminants from wastewater by constructed wetlands: design, performance and mechanism. *Science of the Total Environment* **468–469**, 908–932.

Lv, J. M., Ma, Y. L., Chang, X. & Fan, S. B. 2015 Removal and removing mechanism of tetracycline residue from aqueous solution by using Cu-13X. *Chemical Engineering Journal* **273**, 247–253.

Lv, J. M., Ma, Y. L., Chang, X., Fang, J. Z., Cai, L. Y., Ma, Y. & Fan, S. B. 2017 Chemical adsorption of oxytetracycline from aqueous solution by modified molecular sieves. *Water Science & Technology* **75** (5), 1221–1232.

MacKay, A. A. & Canterbury, B. 2005 Oxytetracycline sorption to organic matter by metal-bridging. *Journal of Environmental Quality* **34**, 1964–1971.

Martínez-Huitle, C. & Ferro, S. 2006 Electrochemical oxidation of organic pollutants for the wastewater treatment: direct and indirect processes. *Chemical Society Reviews* **35**, 1324–1340.

Park, D., Yun, Y. S. & Park, J. M. 2010 The past, present, and future trends of biosorption. *Biotechnology and Bioprocess Engineering* **15**, 86–102.

Parolo, M. E., Baschini, M. T. & Avena, M. J. 2008 Tetracycline adsorption on montmorillonite: pH and ionic strength effects. *Applied Clay Science* **40**, 179–186.

Pils, J. R. V. & Laird, D. A. 2007 Sorption of tetracycline and chlortetracycline on K- and Ca-saturated soil clays, humic substances, and clay-humic complexes. *Environmental Science & Technology* **41**, 1928–1933.

Pulido, J. M. O. 2016 A review on the use of membrane technology and fouling control for olive mill wastewater treatment. *Science of the Total Environment* **563–564**, 664–675.

Raji, C. & Anirudhan, T. S. 1998 Batch Cr(VI) removal by polyacrylamide-graftee sawdust: kinetics and thermodynamics. *Water Research* **32**, 3772–3780.

Salama, T. M. & Ahmed, A. H. 2006 Y-type zeolite-encapsulated copper(II) salicylidene-*p*-aminobenzoic Schiff base complex: synthesis, characterization and carbon monoxide adsorption. *Microporous and Mesoporous Materials* **89**, 251–259.

Shah, A. T., Din, M. I., Kanwal, F. N. & Mirza, M. L. 2015 Direct synthesis of mesoporous molecular sieves of Ni-SBA-16 by internal pH adjustment method and its performance for adsorption of toxic Brilliant Green dye. *Arabian Journal of Chemistry* **8**, 579–586.

Shen, B. J., Qin, Z. X., Gao, X. H., Lin, F., Zhou, S. G., Shen, W., Wang, B. J., Zhao, H. J. & Liu, H. H. 2012 Desilication by alkaline treatment and increasing the silica to alumina ratio of zeolite Y. *Chinese Journal of Catalysis* **33** (1), 152–163.

Wang, Y., Jia, D., Sun, R., Zhu, H. & Zhou, D. 2008 Adsorption and cosorption of tetracycline and copper (II) on montmorillonite as affected by solution pH. *Environmental Science & Technology* **42**, 3254–3259.

Yu, F., Li, Y., Han, S. & Ma, J. 2016 Adsorptive removal of antibiotics from aqueous solution using carbon materials. *Chemosphere* **153**, 365–385.

Zhang, X., Li, R. & Ji, M. 2018 Mechanisms and influencing factors of antibiotic removal in sewage biological treatment. *Environmental Science* **39**, 5276–5288.

First received 10 October 2018; accepted in revised form 25 February 2019. Available online 18 March 2019